NANO LETTERS

Letter

pubs.acs.org/NanoLett

Time-Resolved X-ray Diffraction Investigation of the Modified Phonon Dispersion in InSb Nanowires

A. Jurgilaitis,[†,‡] H. Enquist,[‡] B. P. Andreasson,[†] A. I. H. Persson,[†] B. M. Borg,[⊥,¶] P. Caroff,[§] K. A. Dick,[†,∥] M. Harb,[†,‡] H. Linke,[†] R. Nüske,[†] L.-E. Wernersson,[⊥] and J. Larsson*[,†]

[†]Department of Physics and [‡]MAX IV Laboratory, Lund University, P.O. Box 118, SE-221 00 Lund, Sweden

[§]Department of Electronic Materials Engineering, Research School of Physics and Engineering, The Australian National University, Canberra ACT 0200, Australia

[∥]Division of Polymer and Materials Chemistry, Department of Chemistry and [⊥]Department of Electrical and Information Technology, Lund University, P.O. Box 124, SE-221 00 Lund, Sweden

ABSTRACT: The modified phonon dispersion is of importance for understanding the origin of the reduced heat conductivity in nanowires. We have measured the phonon dispersion for 50 nm diameter InSb (111) nanowires using time-resolved X-ray diffraction. By comparing the sound speed of the bulk (3880 m/s) and that of a classical thin rod (3600 m/s) to our measurement (2880 m/s), we conclude that the origin of the reduced sound speed and thereby to the reduced heat conductivity is that the C_{44} elastic constant is reduced by 35% compared to the bulk material.

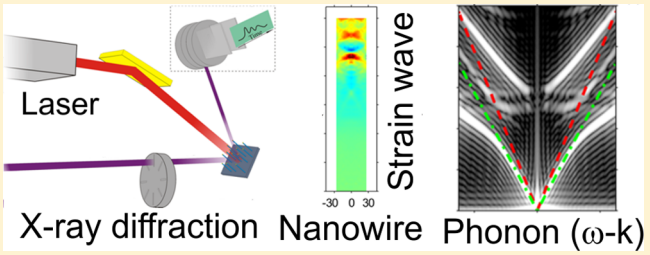

KEYWORDS: *Nanowires, time dependent, X-ray diffraction, elastic properties, thermal conductivity, indium antimonide*

An emerging application of nanostructured materials is in thermoelectrics, where InSb nanowires have been predicted to have desirable properties, including a suppressed thermal conductivity.[1,2] Nanowires are of great interest for diverse applications[3] including nanoelectronics,[4] photonics,[5] and thermoelectrics.[1,2] In each of these applications, the thermal conductivity, κ, of nanowires is of significant consequence for the device performance, either because a high κ is desirable (as is the case for thermal management in photonic and electronic devices) or because a low κ is critical, as is the case for thermoelectric applications.[6] The thermal conductivity is given by

$$\kappa = \frac{1}{3} C l v \tag{1}$$

where C is the specific heat per unit volume, l is the mean free path of the phonons, and v is the speed of sound.[7] All three factors (C, l, and v) can be modified by the length scale of the nanostructure. The specific heat capacity is directly influenced by the phonon density of states, the mean free path is reduced by the small dimensions due to surface scattering, and the speed of sound is reduced by the rod geometry and by the modified elastic constants. The idea to modify heat conductivity by phonon engineering in nanostructures was first presented by Balandin and Wang for a quantum well[8] and later extended to nanowires.[9] A more complete description of phonons in confined systems and the impact of confinement on heat conductivity is presented in a recent review article.[10]

The ideal thermoelectric material has a structure that scatters phonons efficiently without affecting electronic transport. The most investigated material is Si due to its availability and well-known physical properties. It has been both theoretically and experimentally shown that heat transfer in Si nanowires is slower[11] than in the bulk material and is furthermore strongly dependent on the diameter of the nanowire.[12] In general, κ in nanowires is suppressed compared to the corresponding bulk value[13,14] due to an expected modification of the phonon density of states in one dimension and due to diffusive scattering of phonons at the nanowire surface.[2,14,15] It has previously been observed experimentally that heat conduction in thin Si nanowires deviates substantially from the Debye T^3 law, which suggests that changes in phonon dispersion due to confinement could have an appreciable effect.[12] However, experiments that measure κ cannot directly distinguish between these different mechanisms, and in general one has to rely on modeling to understand the measured κ[14]although it has been suggested that the phonon dispersion relation for the confined system plays an important role.[16,17] Here, we measure the acoustic phonon dispersion relation in nanowires using time-resolved X-ray diffraction with high frequency and momentum resolution. We investigate the phonon dispersion of InSb nanowires, which is expected to be the most promising III−V material for thermoelectrics.[15] We show that 50 nm diameter InSb (111) nanowires exhibit a reduced sound speed compared to the bulk, which will result in reduced heat conductivity. The

Received: September 26, 2013
Revised: December 27, 2013
Published: January 3, 2014

   dx.doi.org/10.1021/nl403596b | *Nano Lett.* 2014, 14, 541−546

measurement is performed by generating transient acoustic waves using short laser pulses. The transient waves are built up by coherent acoustic phonons, which can be probed using time-resolved X-ray diffraction.[18] The strength of this method is that it can be used with no special sample preparation on ensembles of as-grown wires for a wide range of materials and diameters. This method has so far only been applied to bulk[18] and multilayered samples.[19,20] The method relies on absorption of short laser pulses to excite the acoustic waves. Short-pulse lasers are available commercially with wavelengths ranging from 190 to 10000 nm making it possible to obtain absorption in almost any material. The second element of the method is time-resolved X-ray scattering, which is available at several synchrotron beamlines.

The experiments were carried out at beamline D611 at the MAX II electron storage ring in Lund, Sweden. The setup is shown in Figure 1 and was described by Harbst et al.[21] Here we give details directly related to this study. The experiments were carried out using X-ray photons with tunable energy around 1.9 keV. A double-crystal InSb monochromator with a bandwidth of $\Delta E/E = 4 \times 10^{-4}$ was used to select the X-ray energy. The X-ray focal spot size was 400 × 200 μm^2 and the divergence was 7 × 0.7 $mrad^2$ (horizontal × vertical). Scattering was carried out in a vertical geometry. The diffraction angle was 59°. In this geometry, the full length of the nanowires was probed. The short laser pulses were generated by a passively mode-locked, titanium-doped sapphire oscillator followed by a cryogenically cooled Ti:Al_2O_3 multipass laser amplifier. The amplifier was operated at a center wavelength of 780 nm, and the pulse duration was 70 fs. The laser system was synchronized to a single electron bunch in the MAX II storage ring. Laser excitation was normal to the surface and the incident laser fluence was 3 mJ/cm^2. The diffracted signal was recorded by a streak camera. The time window of the streak camera was set to 300 ps. In this mode of operation, the temporal resolution is limited to approximately 15 ps.

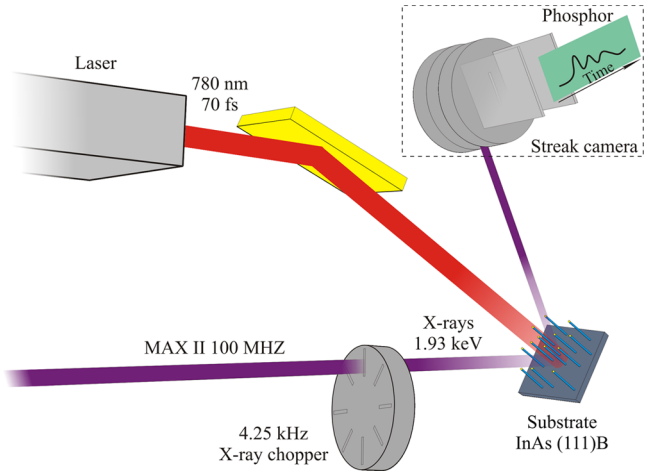

Figure 1. Experimental setup. InSb nanowires grown on an InAs(111) B substrate are excited by femtosecond laser pulses incident normal to the sample and probed by X-rays incident at 59°. Approximately 15 ps time resolution is achieved by using a streak camera detector, hence allowing the detection of coherent acoustic phonons in the excited sample.

The InSb (111)B nanowires[22] investigated in the present study were grown by metalorganic vapor phase epitaxy (MOVPE) using trimethylindium, trimethylantimony, and arsine precursors on an InAs (111)B substrate prepared with gold (Au) nanoparticles. In order to find deviations from the bulk properties, the InSb nanowires were grown as thin as possible. The length was made long enough so that propagation through the wire could be observed over several 100 ps. The length of the InSb nanowires was 1.1 μm and the diameter approximately 50 nm. The density of the nanowires grown on the surface was 5 μm^{-2} and their position on the substrate follows a random distribution. The average diameter for the ensemble of nanowires was measured using small-angle X-ray scattering to be 54 nm. Hence, all simulations were carried out for a diameter of 54 nm. In the paper we refer to the wires as 50 nm.

Coherent phonons were generated by a short (70 fs) laser pulse at a wavelength of 780 nm. The light pulse is absorbed by the nanowire and the energy given to the electrons is transferred to the lattice within a few picoseconds. The energy deposition leads to a temperature rise that results in a thermal stress. The thermal stress develops into a compression strain pulse. This mechanism is discussed in detail by Thomsen et al. for a bulk material.[23] The propagating strain pulse can be considered to consist of a wide spectrum of coherent phonons that can be investigated by time-resolved X-ray diffraction.[18] In

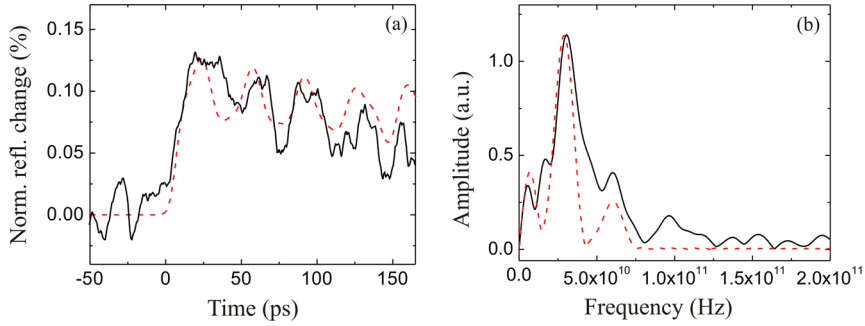

Figure 2. (a) Change in normalized time-resolved X-ray reflectivity from a nanowire with a propagating acoustic wave as measured with the X-ray streak camera. The phonon momentum was 6.5 × 10^7 m^{-1}. The solid black line denotes experimental data and the dashed red line shows a simulation. The dynamical diffraction tool GID_SL on Sergey Stephanov's X-ray server[40] was used to calculate the time-resolved X-ray signal from the time-dependent strain distributions given by the acoustics simulation. Stephanov's X-ray server does not enable calculations for nanowires, so we instead calculated the diffraction pattern from a stack of strained thin films with a total thickness corresponding to the length of the nanowire. The simulated data were convoluted by a 15 ps Gaussian function to give the same time resolution as the experimental data. (b) The corresponding Fourier transform.

dx.doi.org/10.1021/nl403596b | Nano Lett. 2014, 14, 541−546

order to measure each point on the phonon dispersion curve, the X-ray energy is detuned from the optimum scattering condition so that the additional momentum from the phonon is needed to fulfill the Laue condition for scattering[18,24]

$$\mathbf{k}_0 - \mathbf{k}_s = \mathbf{G} \pm \mathbf{q} \quad (2)$$

where $\mathbf{k}_0$ and $\mathbf{k}_s$ are the wave vectors of the incident and scattered X-ray waves respectively, $\mathbf{G}$ is the reciprocal lattice vector, and $\mathbf{q}$ is the phonon wave vector describing the momentum. Because of the scattering geometry, we probe the wave that propagates in in the direction of the probed lattice vector which is the axial (111) direction. We are only sensitive to the longitudinal acoustic modes as Bragg diffraction probes the lattice plane distance. The phonon momentum to be investigated is thus chosen by selecting the X-ray energy. The frequency of the phonon can be measured directly by recording the temporal dependence of the X-ray diffraction intensity and Fourier transformation of the recorded data. Because the frequency of the phonon is measured as a function of momentum, we are effectively generating a point on the dispersion curve. Thus, by carrying out a series of measurements where the probed phonon momentum is changed, the dispersion curve can be reconstructed. For small wavevectors, the acoustic branch is given by $\omega = vq$, where v is the acoustic propagation speed and ω is the phonon angular frequency. Hence, the acoustic propagation speed can be evaluated from the slope of the measured phonon dispersion curve.

In Figure 2a, we show a measurement of the X-ray intensity as function of time for an energy detuning corresponding to a phonon momentum of 6.5×10^7 m^{-1}. Following the initial increase in X-ray signal, an oscillatory pattern from the phonon with the selected momentum is visible. The strength of the method is obvious as the phonon frequency is apparent already in the raw data. In Figure 2b, a Fourier transform of the oscillating X-ray reflectivity is shown. The peak positions give the phonon frequencies with high resolution. The propagation of an acoustic wave in a nanowire is more complex than in bulk material. Because the phonon wavelength is comparable to the dimensions of the nanowire, it acts as an acoustic waveguide and the phonon modes couple to the eigenmodes of the structure. These eigenmodes have oscillation periods ranging from picoseconds to nanoseconds. The fastest one is the fundamental breathing mode.[25] Modes with eigenfrequency on the nanosecond time scale have been investigated using time-resolved X-ray diffraction.[26] In the 50 nm diameter InSb (111) nanowires, the period of the breathing mode is about 19 ps. In this case, an analysis based on eigenmodes is not suitable as they have not had time to develop in the axial direction. For this reason, we carry out simulations of the generation and propagation of the strain waves that are built up by the all-phonon modes.

We used Comsol multiphysics to model both the laser absorption and the acoustic phonon propagation in an InSb nanowire. The simulations were done for a single nanowire in three-dimensions (3D) and divided into two steps. First, the light absorption was calculated by sending a plane wave with a wavelength of 780 nm toward a nanowire standing on a substrate. The simulation takes into account the diffraction from the nanowires with dimensions smaller than the wavelength of the exciting light.[27] More details regarding our simulations of light absorption in nanowires is given in Jurgilaitis et al.[28] The laser that is incident parallel to the axial nanowire direction excites material both on the sides and the top. The electric field direction breaks the symmetry and a deeper penetration with higher excitation is obtained in the direction of the field vector. The resulting absorbed power in the nanowire was then used to calculate the local temperature increase. The rapid temperature increase creates thermal stress. In the second step of the simulation, the resulting strain propagation in the structure was modeled. The propagating axial strain is shown in Figure 3. The complex shape is an

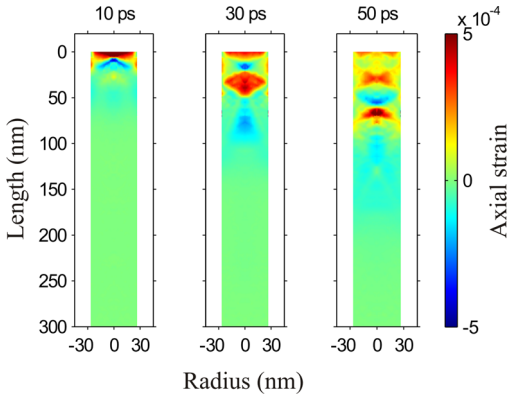

Figure 3. Simulated axial strain in a nanowire 10, 30, and 50 ps after excitation with a short laser pulse. The exciting laser pulses were incident parallel to the axial direction. The colored area corresponds to a radius of 27 nm and the top 300 nm of the nanowire. The strain must start from a free surface and because we are observing axial strain the top surface is the starting point of the axial strain wave. The axial strain that is shown is evaluated in the center plane of the nanowire. The complicated shape of the strain profile shows the strong coupling between the acoustic propagation modes and the radial eigenmodes of the nanowire.

indication of the strong coupling between the propagating wave and the radial eigenmodes. This axial strain profile has been used to calculate the time-resolved X-ray reflectivity curve shown together with the experimental data in Figure 2.

In Figure 4 we plot the phonon frequency as function of momentum for a set of measurements such as the one in Figure 2. The lower branch of the dispersion curve was reconstructed by fitting a line to the experimental points. From the slope of

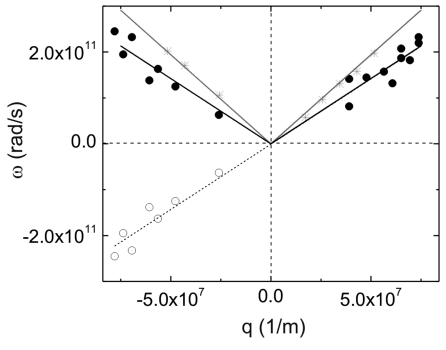

Figure 4. Angular frequency for a set of X-ray reflectivity measurements on nanowires with different phonon momentum ($\mathbf{q}$) (filled circles). The open circles are a geometric mirror of the negative $\mathbf{q}$ data in order to facilitate a fit of a straight line. The slope of the black line corresponds to the sound speed 2880 ± 120 m/s. The gray stars are data points from measurements on bulk InSb. The slope of the gray line gives the bulk sound speed 3860 ± 60 m/s, which is close to the tabulated value of 3880 m/s.

dx.doi.org/10.1021/nl403596b | Nano Lett. 2014, 14, 541−546

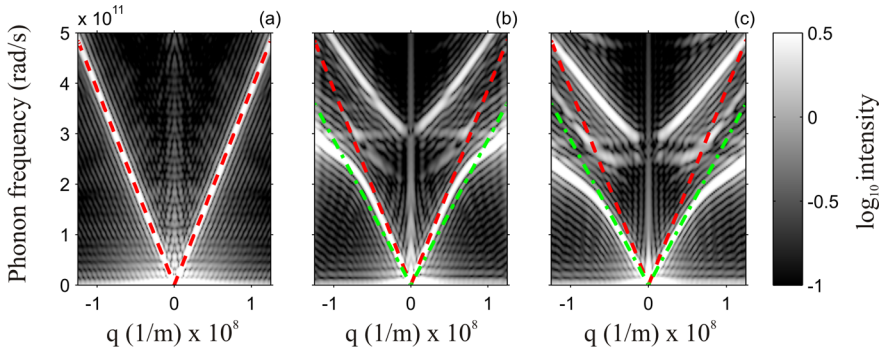

Figure 5. Simulated dispersion relation for (a) bulk InSb. The slope of the dispersion curve is 3880 m/s, which is the bulk speed (b) nanowires with bulk elastic properties, where the slope of the lower acoustic branch corresponds to the rod speed 3600 m/s and (c) nanowires with elastic constants giving the best fit to the experimental sound speed 2880 m/s. The logarithmic intensity scale is shown on the right. The nanowires have a more complex dispersion relation. The lowest branch corresponds to a propagating acoustic wave. The second branch with constant frequency is the breathing mode. The higher branches have a complicated shape due to strong coupling to the eigenmodes of the wire. The red line shown in all three figures corresponds to the sound speed in bulk InSb. The green curve shown in (b,c) corresponds to the measured sound speed in the nanowires. The influence of numerical noise can be seen and identified in the bulk dispersion curve which in absence of such noise is a pure V-shape in this range.

the line, we determined that the strain wave propagates at a speed of 2880 ± 120 m/s for the 50 nm diameter wires, where the error bar is given as a 90% confidence interval for the slope of the fitted line. A measurement of the bulk material is also presented. This measurement was carried out to verify that the slope of the measured bulk dispersion curve is in agreement with the tabulated bulk value.

In Figure 5, we show dispersion curves generated by Fourier transforming the calculated time-resolved strain distribution in time and in space. Thus, the images show the relationship between phonon frequencies and momenta that are excited. The difference between the dispersion curves of the nanowire compared to the bulk can be seen by comparing Figure 5 panel a and b. The dispersion curve for the bulk material has a plain v-shape for low phonon momenta indicating a constant sound speed as function of acoustic phonon frequency. The dispersion curve for the nanowire is more complex due to the wave coupling between the radial eigenmodes and the propagating strain wave. The lowest branch in the simulated dispersion curve for the nanowires (Figure 5b) is acoustic-like and corresponds to the propagation mode observed in the experiment (black line in Figure 4). This branch has a lower slope than the bulk corresponding to a lower propagation velocity as expected for acoustic wave propagation in a thin rod. For 50 nm nanowires, the linear relation of the acoustic branch is valid for phonon momenta up to 7×10^7 m^{-1} (exceeding the inverse of the wire radius). Above this value the lowest branch flattens out. In these simulations, the bulk elastic constants were used. One can also see the relatively flat branch at $\sim 3 \times 10^{11}$ rad/s, which is close to the expected value for the breathing mode. The slope of the lower branch of the simulated dispersion curve shown in Figure 5b yielded a propagation speed of 3600 m/s.

The sound speed in a thin rod is given by

$$v_{\mathrm{rod}} = \sqrt{\frac{Y}{\rho}} \tag{3}$$

where Y is Young's modulus and ρ is the density.[29] Young's modulus for the 111-direction can be calculated using the elastic constants as[32]

$$Y = 3C_{44}\frac{C_{11} + 2C_{12}}{C_{11} + C_{12} + C_{44}} \tag{4}$$

where C_{11}, C_{12}, and C_{44} are the elastic constants. This gives v_{rod} = 3600 m/s, which is in agreement with the simulation result and the tabulated value for thin InSb (111) rods with bulk properties, which also is 3600 m/s.[30,31]

The experimentally obtained acoustic propagation speed 2880 m/s is significantly lower than the value obtained from the simulation and from eqs 3 and 4. This discrepancy can be seen in Figure 5b as a difference of the slope of the high-intensity lower branch in the simulation and the green line that is the fit to the experimental nanowire data from Figure 4. This leads us to the conclusion that the acoustic waveguide effect has a marginal effect on the sound speed and that the explanation for the reduced sound speed in the nanowires compared to that of the bulk material has to be found elsewhere. From eq 4[32] it can be seen that the acoustic propagation speed in the (111) direction depends almost solely on the C_{44} elastic constant[33] making it possible to determine C_{44} by fitting to the data. The influence of the two other independent elastic constants C_{11} and C_{12} is much weaker. In order to determine C_{44} for 50 nm diameter InSb nanowires, we carried out a set of simulations to find the value that best matches the experimentally measured propagation velocity of 2880 m/s. The best fit was obtained when the C_{44} elastic constant was reduced by 35% compared to the bulk as shown in Figure 5c. Thus, we find that the value of C_{44} in the nanowire is 19 ± 2 GPa compared to the bulk value of 30 GPa.

In order to explain the reduction we have carried out an analysis using the core−shell method as discussed in a recent paper by Yao et al.[34] We also compare our finding with theory[34] and measurements on silicon[35,36] that is a material with similar structure to InSb because the diamond structure is a special case of the zinc-blende structure when the two atoms of the unit cell are the same. The core−shell model is a semiempirical model that describes surface elasticity by two parameters. The first is the thickness of the shell and the second is a parameter describing the change of elastic constant in the shell. For silicon, Yao et al. assumes 1 nm shells with a reduction of about a factor 3 in Young's modulus. This is in agreement with molecular dynamics (MD) simulations but a higher value for

dx.doi.org/10.1021/nl403596b | Nano Lett. 2014, 14, 541−546

the radius would be required to match the experimental value of Zhu et al.[35] In order to test this possibility, we carried out simulations using the core−shell geometry where the parameters were modified to reproduce the measured dispersion curves. Given the large diameter of the wire, we used a shell with fixed elastic constant rather than the smoothly changing elastic constant that is needed to reproduce data for small-diameter wires. We found that our core shell model requires a 6 nm thick shell with a reduction of elastic constant of factor 4 in order to obtain a 35% reduction of C_{44}. This thickness is too large to explain the deviation by surface strain. It is common that nanowires (InSb included) grow radially at the same time they are growing axially. The seed gold particles are 40 nm and the wires are 54 nm in width, which is consistent with 7 nm of radial growth. Structurally, it is the same material but the background carbon doping level can be different. Such effects could potentially explain the softening of the material. There is controversy in the scientific community regarding changes of elastic constants in nanowires with wire diameter. It has been suggested that elastic property changes in nanowires with diameter is due to imperfections in growth and experimental conditions.[37] On the other hand, theoretical models and MD simulations predict changes, which are in agreement with other experiments[38,36,39] when it come to the sign of the change (increase or decrease) even though experiments frequently show more dramatic changes.

Previously, a modification of the phonon density of states and the diffusive scattering of phonons at the nanowire surface have been considered as the reason for the reduced heat conductivity in nanowires compared to the bulk material. The origin of the reduced heat conductivity is complex, but our work shows that the reduced elastic constants can be a major contributing factor to the reduced heat conductivity in nanowires compared to the bulk. The ability to directly measure the elastic constants and sound propagation speeds on as-grown wafers will enable screening of materials and optimization of the properties of nanowire-based devices.

AUTHOR INFORMATION

Corresponding Author

*E-mail: jorgen.larsson@fysik.lth.se.

Present Address

¶(B.M.B.) IBM Research − Zürich, Säumerstrasse 4, 8803 Rüschlikon, Switzerland

Author Contributions

A.J. conceived the study, was responsible for all measurements, analyzed the data, and wrote the manuscript. H.E. carried out the simulations on phonon propagation and light absorption in nanowires and analyzed the data. A.I.H.P, R.N., B.P.A., and M.H. participated in the experimental work. H.L., K.D., and L.-E.W. contributed to the discussion. B.M.B. prepared the samples. P.C. and B.M.B. developed the sample preparation method. J.L. conceived the study, supervised the measurements and simulations, and wrote the manuscript.

Notes

The authors declare no competing financial interest.

ACKNOWLEDGMENTS

The authors would like to thank the Swedish Research Council (VR), the Knut and Alice Wallenberg Foundation, the Crafoord Foundation, Stiftelsen Olle Engkvist byggmästare, and the Nanometer Structure Consortium at Lund University (nmC@LU) for financial support. M.H. acknowledges financial support from the Natural Sciences and Engineering Research Council of Canada. We acknowledge the assistance of Dr. Gvidas Astromskas in sample preparation and discussions.

REFERENCES

(1) Hicks, L. D.; Dresselhaus, M. S. *Phys. Rev. B* **1993**, *47* (24), 16631−16634.
(2) Mingo, N. *Appl. Phys. Lett.* **2004**, *84* (14), 2652−2654.
(3) Yang, P. D.; Yan, R. X.; Fardy, M. *Nano Lett.* **2010**, *10* (5), 1529−1536.
(4) Li, Y.; Qian, F.; Xiang, J.; Lieber, C. M. *Mater. Today* **2006**, *9* (10), 18−27.
(5) Yan, R. X.; Gargas, D.; Yang, P. D. *Nat. Photonics* **2009**, *3* (10), 569−576.
(6) Dresselhaus, M. S.; Chen, G.; Tang, M. Y.; Yang, R. G.; Lee, H.; Wang, D. Z.; Ren, Z. F.; Fleurial, J. P.; Gogna, P. *Adv. Mater.* **2007**, *19* (8), 1043−1053.
(7) Ziman, J. M. *Electrons and Phonons: The Theory of Transport Phenomena in Solids*; Clarendon Press: Oxford, 1960; p 554.
(8) Balandin, A.; Wang, K. L. *Phys. Rev. B* **1998**, *58* (3), 1544−1549.
(9) Zou, J.; Balandin, A. *J. Appl. Phys.* **2001**, *89* (5), 2932−2938.
(10) Balandin, A. A.; Nika, D. L. *Mater. Today* **2012**, *15* (6), 266−275.
(11) Hochbaum, A. I.; Chen, R. K.; Delgado, R. D.; Liang, W. J.; Garnett, E. C.; Najarian, M.; Majumdar, A.; Yang, P. D. *Nature* **2008**, *451* (7175), 163−U5.
(12) Li, D. Y.; Wu, Y. Y.; Kim, P.; Shi, L.; Yang, P. D.; Majumdar, A. *Appl. Phys. Lett.* **2003**, *83* (14), 2934−2936.
(13) Boukai, A. I.; Bunimovich, Y.; Tahir-Kheli, J.; Yu, J. K.; Goddard, W. A.; Heath, J. R. *Nature* **2008**, *451* (7175), 168−171.
(14) Zhou, F.; Moore, A. L.; Bolinsson, J.; Persson, A.; Froberg, L.; Pettes, M. T.; Kong, H. J.; Rabenberg, L.; Caroff, P.; Stewart, D. A.; Mingo, N.; Dick, K. A.; Samuelson, L.; Linke, H.; Shi, L. *Phys. Rev. B* **2011**, *83*, 205416.
(15) Mingo, N. *Appl. Phys. Lett.* **2006**, *88* (14), 149902.
(16) Mingo, N.; Broido, D. A. *Phys. Rev. Lett.* **2004**, *93*, 246106.
(17) Balandin, A. A. *Nat. Mater.* **2011**, *10* (8), 569−581.
(18) Lindenberg, A. M.; Kang, I.; Johnson, S. L.; Missalla, T.; Heimann, P. A.; Chang, Z.; Larsson, J.; Bucksbaum, P. H.; Kapteyn, H. C.; Padmore, H. A.; Lee, R. W.; Wark, J. S.; Falcone, R. W. *Phys. Rev. Lett.* **2000**, *84* (1), 111−114.
(19) Sondhauss, P.; Larsson, J.; Harbst, M.; Naylor, G. A.; Plech, A.; Scheidt, K.; Synnergren, O.; Wulff, M.; Wark, J. S. *Phys. Rev. Lett.* **2005**, *94*, 125509.
(20) Bargheer, M.; Zhavoronkov, N.; Gritsai, Y.; Woo, J. C.; Kim, D. S.; Woerner, M.; Elsaesser, T. *Science* **2004**, *306* (5702), 1771−1773.
(21) Harbst, M.; Hansen, T. N.; Caleman, C.; Fullagar, W. K.; Jönsson, P.; Sondhauss, P.; Synnergren, O.; Larsson, J. *Appl. Phys. A: Mater. Sci. Process* **2005**, *81* (5), 893−900.
(22) Caroff, P.; Messing, M. E.; Borg, B. M.; Dick, K. A.; Deppert, K.; Wernersson, L. E. *Nanotechnology* **2009**, *20* (49), 495606−495606.
(23) Thomsen, C.; Grahn, H. T.; Maris, H. J.; Tauc, J. *Phys. Rev. B* **1986**, *34* (6), 4129−4138.
(24) Larsson, J.; Allen, A.; Bucksbaum, P. H.; Falcone, R. W.; Lindenberg, A.; Naylor, G.; Missalla, T.; Reis, D. A.; Scheidt, K.; Sjogren, A.; Sondhauss, P.; Wulff, M.; Wark, J. S. *Appl. Phys. A: Mater. Sci. Process* **2002**, *75* (4), 467−478.
(25) Hu, M.; Wang, X.; Hartland, G. V.; Mulvaney, P.; Juste, J. P.; Sader, J. E. *J. Am. Chem. Soc.* **2003**, *125* (48), 14925−14933.
(26) Mariager, S. O.; Khakhulin, D.; Lemke, H. T.; Kjaer, K. S.; Guerin, L.; Nuccio, L.; Sorensen, C. B.; Nielsen, M. M.; Feidenhans'l, R. *Nano Lett.* **2010**, *10* (7), 2461−2465.
(27) Wu, P. M.; Anttu, N.; Xu, H. Q.; Samuelson, L.; Pistol, M. E. *Nano Lett.* **2012**, *12* (4), 1990−1995.
(28) Jurgilaitis, A.; Enquist, H.; Harb, M.; Dick, K. A.; Borg, B. M.; Nüske, R.; Wernersson, L.-E.; Larsson, J. *Struct. Dyn.* **2014**, *1*, 014502.

(29) Bajaj, N. K. *The Physics of Waves and Oscillations*; Tata McGraw-Hill: New Delhi, India, 1984.
(30) Slutsky, L. J.; Garland, C. W. *Phys. Rev.* **1959**, *113* (1), 167−169.
(31) Ashby, M. F.; Ferreira, P. J. S. G.; Schodek, D. L. *Nanomaterials, Nanotechnologies and Design: An Introduction for Engineers and Architects*; Butterworth-Heinemann: Amsterdam, 2009; pp xix−540.
(32) Adachi, S. *GaAs and Related Materials: Bulk Semiconducting and Superlattice Properties*; World Scientific: Singapore, 1994; pp xix−675.
(33) When evaluating eqs 3 and 4 it can be seen that a change of a factor 2 of either C11 or C12 would only change the sound speed by 3%, therefore it is not possible to evaluate C11 or C12 using the data at hand.
(34) Yao, H. Y.; Yun, G. H.; Bai, N. S.; Li, J. G. *J. Appl. Phys.* **2012**, *111*, 083506.
(35) Zhu, Y.; Xu, F.; Qin, Q. Q.; Fung, W. Y.; Lu, W. *Nano Lett.* **2009**, *9* (11), 3934−3939.
(36) Li, X. X.; Ono, T.; Wang, Y. L.; Esashi, M. *Appl. Phys. Lett.* **2003**, *83* (15), 3081−3083.
(37) Rohlig, C. C.; Niebelschutz, M.; Brueckner, K.; Tonisch, K.; Ambacher, O.; Cimalla, V. *Phys. Status Solidi B* **2010**, *247* (10), 2557−2570.
(38) Chen, C. Q.; Shi, Y.; Zhang, Y. S.; Zhu, J.; Yan, Y. J. *Phys. Rev. Lett.* **2006**, *96*, 075505.
(39) Wang, Y. B.; Wang, L. F.; Joyce, H. J.; Gao, Q. A.; Liao, X. Z.; Mai, Y. W.; Tan, H. H.; Zou, J.; Ringer, S. P.; Gao, H. J.; Jagadish, C. *Adv. Mater.* **2011**, *23* (11), 1356−1360.
(40) Stephanov, S. *Advances in Computational Methods for X-ray and Neutron Optics*; Sanches del Rio, M., Ed.; Proceedings SPIE; SPIE Press: 2004; Vol. *5536*, pp 16−26.